A Real-Time Internal Calibration Method for Radar Systems Using Digital Phase Array Antennas

Hung Tran Viet and Thien Hoang Minh(✉)

Le Quy Don Technical University, 236 Hoang Quoc Viet, Hanoi, Vietnam
thienhm.isi@lqdtu.edu.vn

Abstract. This paper proposed a real-time internal calibration method for receiving channels of radar systems using phased array antennas with real-time digital beam-forming. In most calibration methods, the frequency of the calibration signal (CalSig) is different from that of the echo signal, leading to some disadvantages in the calibration procedure. This paper analyzed and proposed a novel solution to solve those disadvantages. In the solution, we use the CalSig with the same frequency as the echo signal. The CalSig is a binary phase-shift keying (BPSK) signal and amplitude-modulated by an on-off keying (OOK) code sequence. The proposed CalSig has peak power equivalent to noise power but its average power is much lower than noise power by using OOK modulation with a small duty cycle D such that it does not affect the echo signal significantly. Measurement of receiving parameters is based on correlation properties of the signal. The performance of the proposed method is analyzed using the statistical theory and verified by Matlab simulation. Results show the effectiveness of the method with high accuracy, satisfying the real-time requirement while affecting receiving quality insignificantly. Phase and amplitude errors can be achieved values below 0.5° and 0.2 dB, respectively.

Keywords: Phased array antenna · Real-time calibration · Radar system · Digital beam-forming

1 Introduction

Nowadays, phased array antennas are used widely in radar applications because they have many advantages over the previous systems such as highly spatial selection ability, good interference suppression, high-speed beam scanning, SNR improvement [1]. Systems using the phased array antennas also have more demands about the number of transceiver modules (TRM), directional error, real-time digital beam scanning, etc. Therefore, monitoring amplitude and phase differences between channels is required with higher accuracy. Because parameters of the channels vary continuously under the impacts of aging, temperature and many other factors, real-time monitoring of channel parameters is compulsory. Most of the conventional periodic calibration methods have

N.-S. Vo et al. (Eds.): INISCOM 2021, LNICST 379, pp. 88–103, 2021.
https://doi.org/10.1007/978-3-030-77424-0_8

become inappropriate as they do not meet the real-time specification [2–10]. Thus, a real-time approach of calibration is demanded. Real-time calibration is necessary especially for systems that require monitoring parameters with high accuracy during operation, the process of parameter calibration does not interrupt the operation of the systems. In [11–15], the structure and algorithm of the real-time internal calibration were described clearly for 5G communications or SweepSar radars. In general, calibration procedures presented in those papers are based on coupling to receiving channels a single-tone signal, its frequency is in-band of the receivers but different from echo signal frequency. The echo signal and the CalSig after digitizing will be separated by digital filters, parameters of receiving channels are determined by measuring parameters of the CalSig, the results will be used to complement phase and amplitude differences between channels.

Nevertheless, calibration frequency must be near and far enough from operation frequency. Being near enough to get the best results of calibration and far enough to avoid interference for the echo signal. How near and far the calibration frequency depends on the range of operational frequencies and bandwidth of the system. In [11], the calibration structure was proposed for 5G systems with the frequency range of 27–29 GHz, the difference between the calibration frequency and the operation frequency is 2 MHz. The experiment showed good results with 0.9° phase error and 0.5 dB amplitude error. However, for systems with the spectrum spread principle, signal bandwidth can be up to several tens MHz [16], the errors might be much higher. Obviously, the method in the paper provided experiment results with a simple structure of the signal, which is not appropriate for systems with large signal bandwidth.

In [12–15], real-time calibration was applied on the SweepSar radar with the operating frequency range of 1215 MHz–1300 MHz. The gain-frequency characteristic of its receiver module over temperature is shown in Fig. 1 [15].

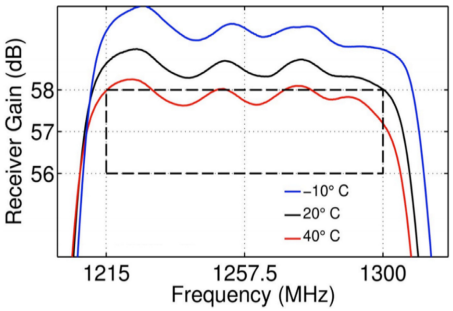

Fig. 1. Gain vs. frequency characteristic with different temperatures.

The above characteristic shows that the gain of the receiving channel is not flat over the range of operational frequencies, the ripple is larger than 0.5 dB and varies with different temperatures. This effect is typical because the specifications of electronic components change over frequency and temperature. Thus, when the calibration frequency is different from the operational frequency and the characteristics of receivers are unknown, determining receiving channel parameters by measuring parameters of the CalSig might lead to significant errors. Similarly, the phase-frequency characteristics are

non-linear and also different from channel to channel, the phase differences can be up to several degrees. These differences are unavoidable, we cannot reduce these errors by measuring multiples times and averaging them. For systems with high accuracy requirements, these errors must be suppressed by characterizing all receiver modules in the whole frequency and temperature range, then set up lookup tables to compensate errors when calibrating in real-time. For systems with a large number of modules, this method is very difficult to realize. We need to arrange sensors to acquire exactly desired temperatures of the modules with the real-time requirement. These solutions demand expensive effort to implement and increase system complexity when the number of modules is large.

To cope with the disadvantages of internal calibration methods, in which frequencies of the CalSig and echo signal are different as mentioned above, we propose a novel calibration scheme with frequencies of the CalSig and echo signal are the same. In Sect. 2, the structure of the CalSig is proposed. Section 3 analyzes measurement errors and the impact of the CalSig on the quality of the system. Verification by Matlab simulation is presented in Sect. 4 and the last one is the conclusion.

2 Structure of the CalSig

In this paper, we select an internal calibration method as presented in [11–15] and focus on receiver calibration. The structure of a TRM according to this calibration method is shown in Fig. 2, including paths of the signals in the receive-and-calibration mode. In this mode, the signal generator will generate the CalSig (blue) to input the RF port of the TRM, the SW1 switch directs the CalSig to the RS and CR connectors. Then the CalSig will be fed to the input of a directional coupler. The CalSig will enter the entire receiving channel together with the echo signal (red) from the antenna. The pink line indicates the combined signal of the CalSig and the echo signal. The high-frequency signal in the receiving channel is down-converted to an intermediate frequency (IF), digitized by an analog-to-digital converter (ADC).

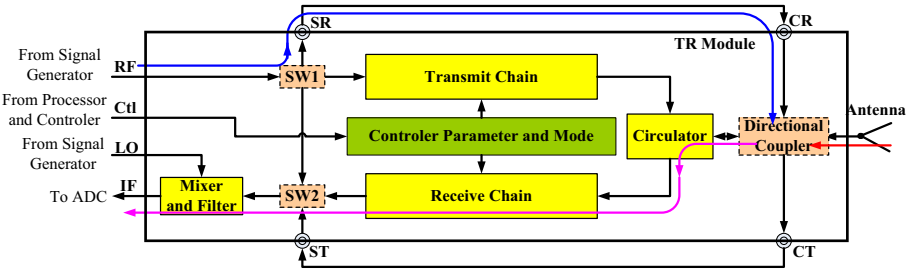

Fig. 2. Structure of a TRM with the signal paths in receiving-and-calibration mode. (Color figure online)

To overcome the disadvantages of the calibration method outlined in [11–15], we propose a solution that the CalSig frequency and the echo signal frequency are equal. The

CalSig is shifted by 180° in phase from pulse to pulse according to a random binary code sequence $C(n) = e^{\pm j\theta} = \pm 1$ ($\theta = 0°$ or 180°) such that the bandwidth of the CalSig and the echo signal is equivalent. It means that the CalSig and the echo signal exist simultaneously in the entire receiving channel including both analog and digital signal processing parts. The IF signal after the ADC does not need digital filters to separate the CalSig and the echo signal as in [11–15], it is demodulated down to baseband (DDC) to produce a quadrature complex signal. This complex signal is a combination signal (ComSig) consisting of three components: the CalSig, the echo signal and the internal noise. In which the CalSig contains phase and amplitude information of the receiving channel. When performing calibration, the ComSig is sampled in the time the OOK modulation code equals "1" and stored in buffers along with the sequence C(n). By correlating the ComSig sample sequence with the C(n) phase code sequence, we obtain the amplitude and phase of the receiving channel. These parameters are used to compensate for phase and amplitude errors between the receiving channels.

When two signals have the same frequency and bandwidth, the determination of the channel parameters through measuring the CalSig will be more accurate. Nonetheless, it leads to interference between two signals, affecting calibration performance and quality of the echo signal processing. Following we will describe solutions to solve these two problems.

The first problem is to ensure the quality of echo signal processing, the CalSig must have a very low average power [17]. However, the ADCs have a limited number of bits and internal noise in radar receivers occupies only several LSB bits, the small echo signal even occupies only 1–2 LSB bits. If we reduce the peak power of the CalSig so that it is much smaller than the noise level, the CalSig may be less than the value of the LSB bit of ADC. Therefore, we choose the CalSig with the peak power equivalent to noise power and amplitude-modulated according to an OOK code with a small duty cycle D, in which the value "1" appears randomly. Then, the average power of the CalSig is much lower than the noise power. The selection of the value of D and the significance of CalSig generation will be analyzed in Sect. 3. The CalSig is illustrated in Fig. 3 with $D = 1/16$.

The second problem is to ensure calibration performance. We have known that the echo signal in the radar receiver appears randomly. When the echo signal is large, the calibration quality will be impacted. To solve this problem, we use a threshold detector for the ComSig in the receiver, when it exceeds an arbitrary threshold, the ComSig is not sampled (although the CalSig is still present in the receiving channel). Threshold selection will be analyzed in Sect. 3, it depends on the requirement of measurement errors. Figure 4 illustrates different situations of the echo signal, if the echo signal is much higher than the noise level, the CalSig is not sampled and stored.

From the above discussions, we can formulate the process of generating the CalSig, measuring parameters and calibrating the receiving channels as shown in Fig. 5.

In Fig. 5, the CalSig is applied to the receiving channel, combined with the echo signal, then passes to ADC and DDC. The ComSig is divided into 3 branches. The noise power measuring unit and the ComSig power measuring unit are used to filter and reject samples with large echo signals. Then, the ComSig is registered into buffers along with

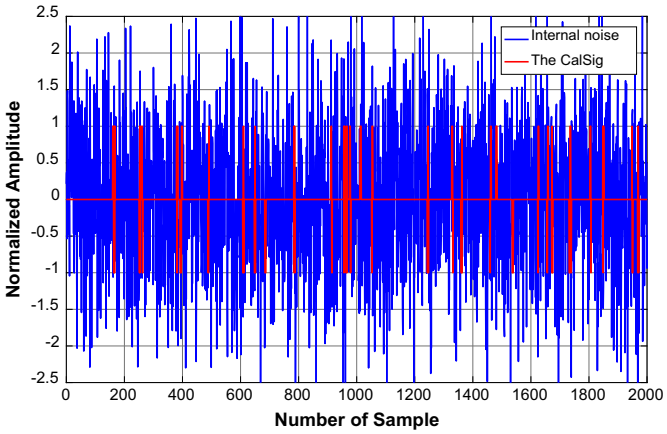

Fig. 3. The CalSig (red) and system noise (blue). (Color figure online)

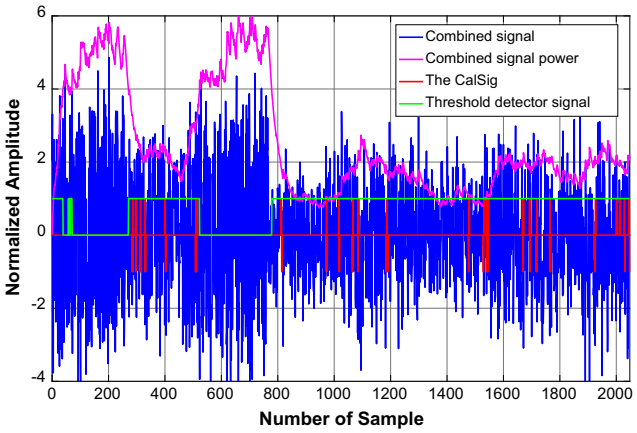

Fig. 4. The CalSig (red) is disable when the echo signal is larger than the threshold. (Color figure online)

the C(n) sequence. When the required set of N samples is sufficient, the correlation processing and receiving channel parameter estimation is performed. Phase and amplitude parameters of all receiving channels are sent to the calibration unit to compensate for channel errors. The theoretical basis for the selection of CalSig modulation parameters is analyzed in detail in Sect. 3.

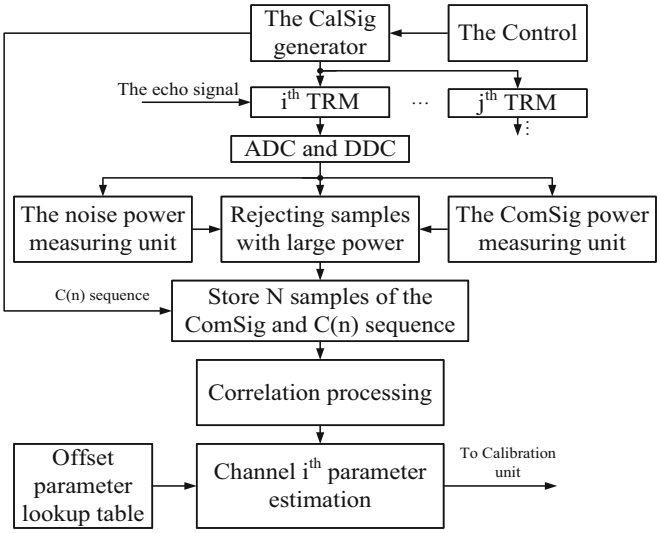

Fig. 5. Measurement and calibration procedure for the receiving channels.

3 Analyzing Measurement Errors and the Impact of the CalSig on the Quality of the System

3.1 Analyzing Measurement Errors

Three types of signals in the receiving channel are illustrated in Fig. 6. The n^{th} sample of the ComSig is represented as follows:

$$S_{Comb}(n) = S_{Cal}(n) + S_{Echo}(n) + N(n) \tag{1}$$

where $S_{Cal}(n) = Ae^{j\varphi}C(n)$ is the CalSig, φ and A denote phase and amplitude of the receiving channel, C(n) = ± 1 is the BPSK modulation code sequence. $N(n) = N_I(n) + jN_Q(n)$ is the internal noise and $S_{Echo}(n) = S_{IEcho}(n) + jS_{QEcho}(n)$ is the echo signal. Assume that $S_{NEcho}(n)$ is a combination of the echo signal and the internal noise:

$$S_{NEcho}(n) = S_{Echo}(n) + N(n) = S_{INEcho}(n) + jS_{QNEcho}(n)$$

$$S_{Comb}(n) = S_{Cal}(n) + S_{NEcho}(n) \tag{2}$$

The C(n) sequence is known, multiplying two sides of (2) by C(n), we obtain:

$$\begin{aligned} S_{Comb}(n)C(n) &= S'_{Comb}(n) = S_{Cal}(n)C(n) + S_{NEcho}(n)C(n) \\ &= Ae^{j\varphi} + S_{INEcho}(n)C(n) + jS_{QNEcho}(n)C(n) \\ &= Ae^{j\varphi} + (S'_{INEcho}(n) + jS'_{QNEcho}(n)) \end{aligned} \tag{3}$$

where C(n) is a binary stochastic sequence with zero expectation, therefore the sequences $S'_{INEcho}(n) = S_{INEcho}(n)C(n)$ and $S'_{QNEcho}(n) = S_{QNEcho}(n)C(n)$ are also

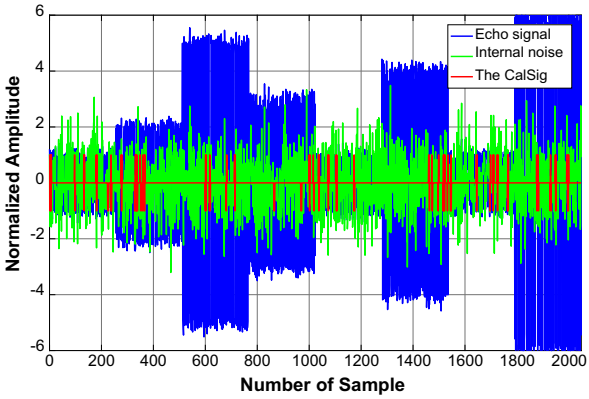

Fig. 6. Illustrate three types of signals in the receiving channel.

stochastic with zero expectation according to [18]. These two sequences have zero expectation for any echo signals $S_{Echo}(n)$. From (3), it can be realized that $S'_{Comb}(n)$ contains phase and amplitude information of the receiving channel in $Ae^{j\varphi}$ expression, while the complex component $S'_{INEcho}(n) + jS'_{QNEcho}(n)$ is the factor causing measurement errors. Define that σ^2_{INEcho} and σ^2_{QNEcho} are variances of the sample sequences $S'_{INEcho}(n)$ and $S'_{QNEcho}(n)$, respectively. In general, measurement error is determined by 3 times standard deviation, then $S'_{Comb}(n)$ is presented with measurement error as follows:

$$S'_{Comb}(n) = Ae^{j\varphi} \pm (3\sigma_{INEcho} + j3\sigma_{QNEcho}) \tag{4}$$

We have known that the random error decreases when averaging over many observations [18], averaging over N observations, the standard deviation decreases by $\sqrt{N}$. Considering the mean of N samples $S'_{Comb}(i), i = 1 \div N$, we obtain:

$$\begin{aligned} \overline{S'_{Comb}} &= Ae^{j\varphi} \pm (3\sigma_{INEcho} + j3\sigma_{QNEcho})/\sqrt{N} \\ &= (Acos\varphi \pm 3\sigma_{INEcho}/\sqrt{N}) + j(Asin\varphi \pm 3\sigma_{QNEcho}/\sqrt{N}) \end{aligned} \tag{5}$$

According to (5), $3\sigma_{INEcho}/\sqrt{N}$ and $3\sigma_{QNEcho}/\sqrt{N}$ are two factors causing errors. The amplitude and phase errors depend on the relationship between φ and two above error components. In this work, without loss of generality, by supposing that $\sigma_{INEcho} = \sigma_{QNEcho} = \sigma_{NEcho}$, we have:

$$\overline{S'_{Comb}} = Ae^{j\varphi} \pm 3\sigma_{NEcho}(1 + j)/\sqrt{N} \tag{6}$$

To facilitate transformation, we suppose that peak power of the CalSig (equivalent to noise power) equals 1 ($A^2 \approx 2\sigma^2_N = 1$), then $2\sigma^2_{NEcho}(2\sigma^2_{NEcho} \geq 1)$ indicates the ratio of the receiving channel power to the CalSig power, transform (6) we acquire:

$$\overline{S'_{Comb}} = e^{j\varphi} \pm 3\sigma_{NEcho}(1 + j)/\sqrt{N} = e^{j\varphi} \pm (3\sqrt{2}\sigma_{NEcho}/\sqrt{N})e^{j\pi/4}$$

Considering the following expression:

$$BT = \overline{S'_{Comb}}/e^{j\varphi} = 1 \pm \frac{3\sqrt{2}\sigma_{NEcho}}{\sqrt{N}} cos(\frac{\pi}{4} - \varphi) \pm \mathrm{j}\frac{3\sqrt{2}\sigma_{NEcho}}{\sqrt{N}} sin(\frac{\pi}{4} - \varphi) \quad (7)$$

Thus, BT is the basis for evaluating the measurement errors of the phase and amplitude of the receiving channel with two variables N and σ_{NEcho}. From (7), the amplitude error is given by:

$$amplitude\_error = |BT|^2 = (1 + 18\sigma^2_{NEcho}/N \pm 6\sqrt{2}\sigma_{NEcho} cos(\pi/4 - \varphi)/\sqrt{N})$$

We only consider the case of the largest error, i.e. $\pm cos(\pi/4 - \varphi) = 1$, then the amplitude error in dB is given by:

$$amplitude\_error\_dB = 10\lg(1 + 18\sigma^2_{NEcho}/N + 6\sqrt{2}\sigma_{NEcho}/\sqrt{N}) \quad (8)$$

Illustrating the Eq. (8) with the power levels of S_{NEcho}, $P(S_{NEcho}) = 2\sigma^2_{NEcho} = 1, 2, 4, 8$, the number of samples $N = 5000 \div 100{,}000$ gives the results as shown in Fig. 7.

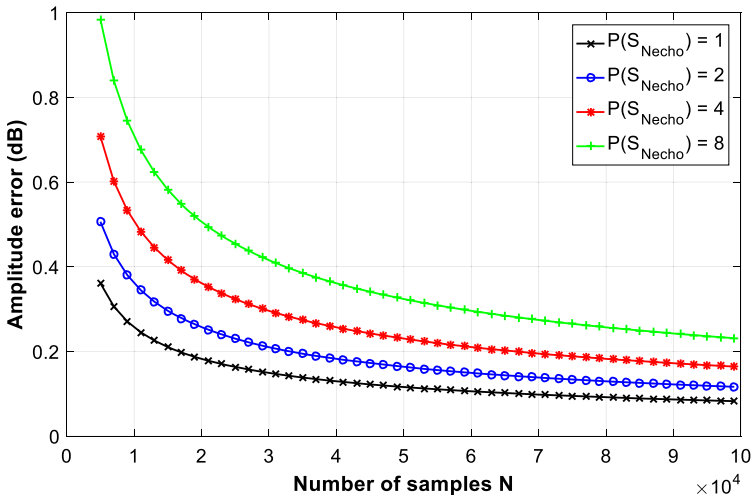

Fig. 7. Amplitude error vs. N with different values of $P(S_{NEcho})$.

Similarly, the phase error is:

$$phase\_error = \Delta\varphi = |Arg(BT)|$$

We only consider the case of the largest error, i.e. $\pm sin(\pi/4 - \varphi) = 1$, then:

$$phase\_error = \Delta\varphi = |Arg(1 + \mathrm{j}\frac{3\sqrt{2}\sigma_{NEcho}}{\sqrt{N}})| \quad (9)$$

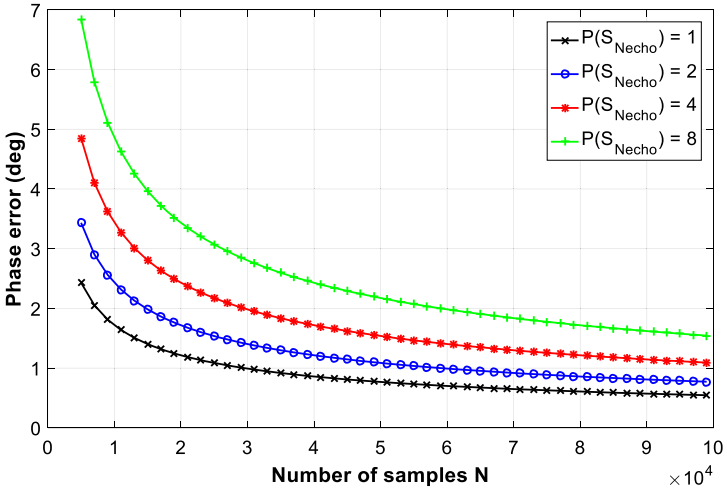

Fig. 8. Phase error vs. N with different values of $P(S_{NEcho})$.

Illustrating the Eq. (9) with the power levels of S_{NEcho}, $P(S_{NEcho}) = 2\sigma^2_{NEcho} = 1, 2, 4, 8$, the number of samples $N = 5000 \div 100{,}000$ gives the results as shown in Fig. 7.

Expressions (8), (9), and Fig. 7, Fig. 8 provide evaluation results of amplitude and phase errors of the receiver channel with the proposed calibration method. It is clear that the larger number of accumulated samples (N) and the smaller echo signal power is, the higher accuracy is. Conversely, the larger echo signal power is, the larger the measurement error is, therefore detecting a large echo signal power and removing the CalSig as described in Sect. 2 will improve measurement accuracy. Depending on requirements of accuracy and calibration time, the threshold value and the number of samples (N) are selected appropriately.

3.2 Impact of the CalSig on the Quality of Receiving Channels

In two previous sections, we have analyzed the problem of measurement errors caused by noise and echo signals when calibrating. In contrast, the CalSig also interferes with the receiving channel, affecting the quality of the receiver. As described in Sect. 2, the CalSig is a BPSK modulated signal, combined with the OOK modulation (Fig. 9a). It has been known that in pulse radar engineering, the signal is typically processed averagely over cycles of repetition. Figure 9b illustrates that the signals are averaged over some cycles. Hence, putting the CalSig with the duty cycle D to the receiving channel is equivalent to applying a continuous CalSig with an average power reduced by $M = 1/D$. In this case, interference in the receiving channel includes the CalSig and internal noise. Calculation of probability distribution function of signals gives results as shown in Fig. 10.

As we can see, the probability density function of interference has a normal distribution with a standard deviation σ_N. σ_N decreases if M increases, when $M = 4, 8, 16, 32$, value of σ_N is 1,118, 1,061, 1,031, 1,016 and power of the interference increases by

0.97, 0.51, 0.26, 0.13 (dB), respectively. It is clear that when M = 32, the interference power increases negligibly (0.13 dB). To evaluate more comprehensively the impact of the CalSig on the quality of the receiver, we calculate for an active radar system. In a radar system, the most important parameter is the detection range. The relationship of the maximum detection range R_{max}, sensitivity P_{min} and noise power P_N of the receiver is described by the following expression:

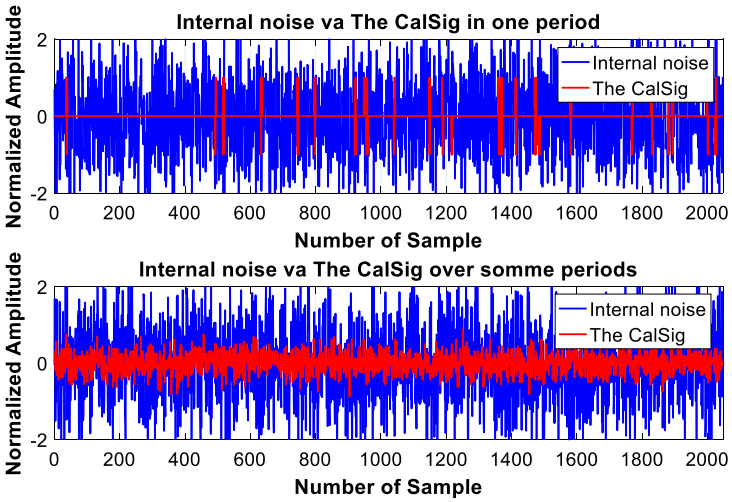

Fig. 9. The CalSig in one period and over some periods.

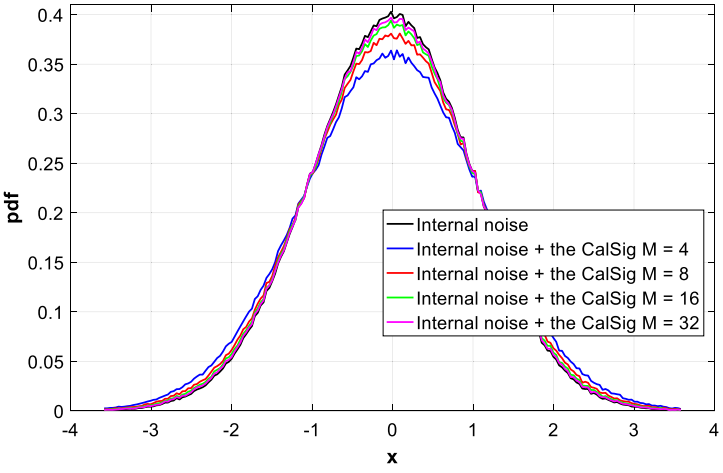

Fig. 10. Probability density function of interference with and without the CalSig.

$$P_{Rmin} = \frac{A}{R_{Max}^4} = P_N \cdot SNR_{Min} \tag{10}$$

where SNR_{min} determines the value of true detection probability and false alarm probability. When the CalSig is applied to the receiving channel, expression (10) is rewritten as:

$$P_{RminCal} = \frac{A}{R^4_{MaxCal}} = P_{NCal} \cdot SNR_{Min} \tag{11}$$

From (10) and (11), we obtain:

$$R_{MaxCal}/R_{Max} = \sqrt[4]{P_N/P_{NCal}} = \sqrt[4]{M/(M+1)} \tag{12}$$

The graph representing the ratio R_{MaxCal}/R_{Max} (%) vs. M is shown in Fig. 11.

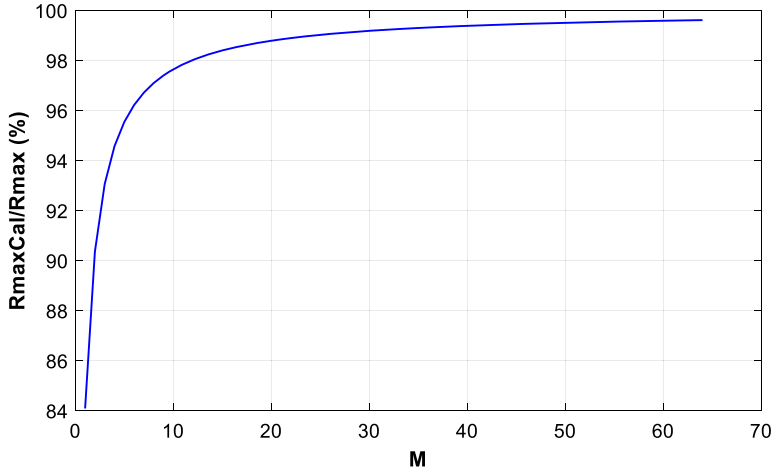

Fig. 11. R_{maxCal}/R_{max} vs. blank ratio M.

The result indicates that when M > 24 (D < 4.2%) the ratio R_{maxHC}/R_{max} exceeds 99%. Thus, the proposed CalSig provides good calibration results and its impact on the detection range of the radar is negligible with a small value of D.

It is obvious that the proposed calibration method will take a long processing time because the required number of samples N is large. In addition, during the time that the echo signal exceeds the threshold, sampling the ComSig must be paused. The following example illustrates the time duration necessary to acquire a sufficient number of samples. With phase and amplitude errors are required below 1° and 0.2 dB, we need a number of samples: N = 131,072 (2^{18}) over some receiving/transmiting cycles, the blank ratio of the CalSig: M = 32, a cycle has 2048 range cells. Then through about 1600 cycles, we will have enough N samples. Suppose that in half of a cycle, the echo signal exceeds the threshold at which the ComSig is not sampled, therefore we need 3200 receiving/transmiting cycles. If each cycle is about 1 ms, then after 3.2 s, N samples will be acquired entirely. That time completely meets the real-time requirement of the calibration for radar systems. Parameters of electronic components in the operational process mainly vary due to temperature, this change is relatively slow, even performing

calibration in a few tens of seconds still meets the real-time requirement. Hence, to improve the measurement accuracy, we can increase the number of samples (N), particularly if the phase and amplitude errors are required below 0.5° and 0.1 dB, we need to acquire $N = 2^{20}$ samples.

4 Evaluation of the Proposed Calibration Method by Simulation

In this section, we verify the proposed calibration method by Matlab simulation for independent receiving channels of a radar system using digital beamforming. Assume that the system has four receiving channels with different phase and amplitude (gain) parameters, the phase parameters are 0, 60, 120, 180 degrees and the amplitudes are 0, 1.58, 2.92, 4.08 dB, respectively. The echo signals on the receiving channels are segments of random signals in the time domain with a random level in the range of 0–5 in comparison to the noise level. The CalSig has $M = 32$, peak power equivalent to the noise level (Noise has the normal distribution). Since the CalSig average power is very low, the ComSig power is considered to be approximately equal to the S_{NEcho} signal power. The threshold level of the ComSig power to stop sampling is four times the noise power (6 dB), the required number of samples is $N = 100{,}000$. Each calibration process is started when we have enough N samples, calculating the phase and the amplitude errors of the channels, compensating for those errors, then continuing to acquire N samples for the next calibration. Results before and after calibration are shown in Figs. 12 and 13.

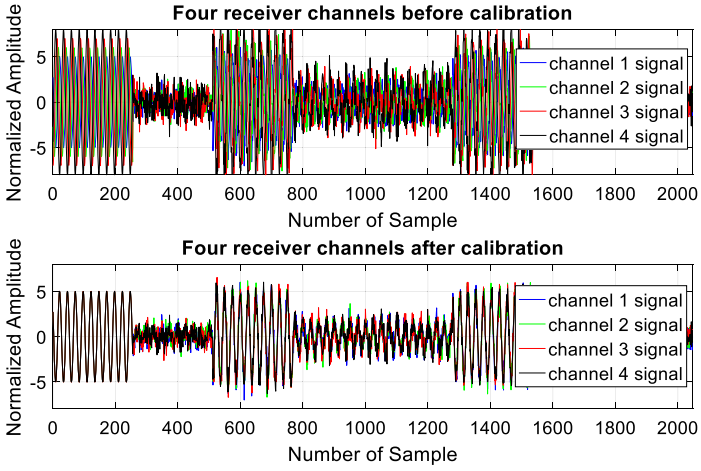

Fig. 12. Signals in receiving channels before and after calibration.

It is clear that after calibration, signals at the outputs of the receiving channels have the same phase and amplitude. The phase and amplitude errors of the channels in comparison with the first channel are shown in Figs. 14. The measurement results were recorded after each calibration. Figures 14 indicates errors of 100 calibrations. The results show that the amplitude and phase errors are smaller than 0.1 dB and 0.8°, respectively.

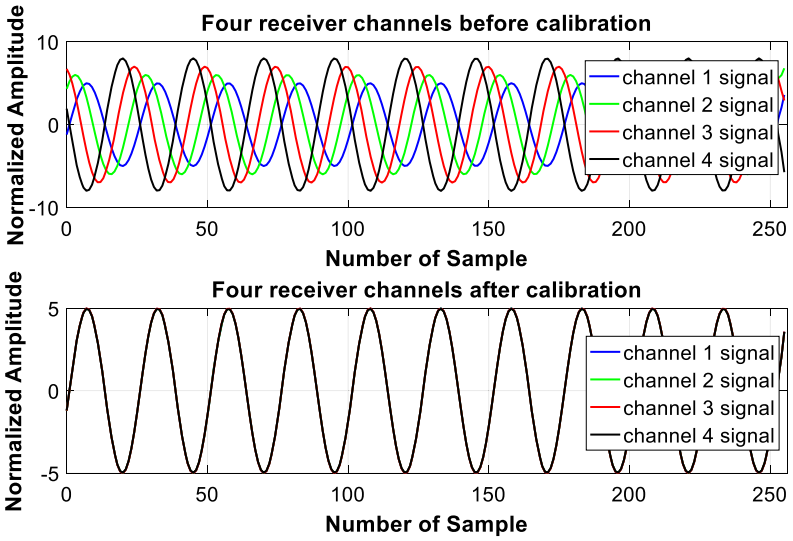

Fig. 13. Signals in receiving channels before and after calibration (Zoom out).

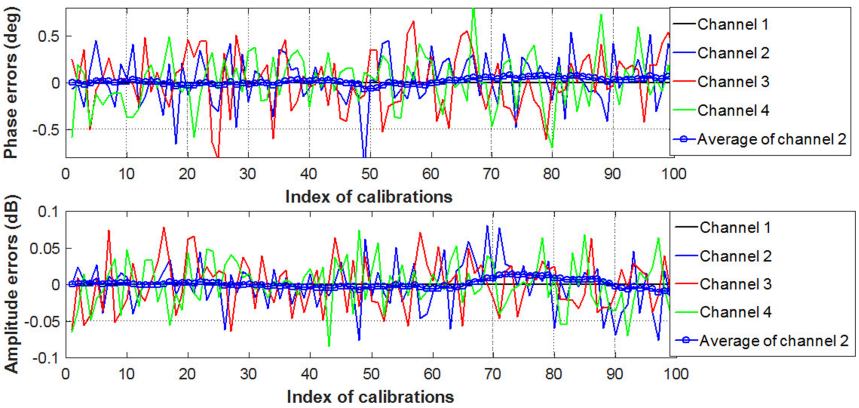

Fig. 14. Phase and amplitude error after calibration.

The calibration method presented in [11] achieves experimental results with a phase error of 0.9° and amplitude error of 0.5 dB. Result comparison shows that the proposed solution is feasible, achieving high accuracy in phase and amplitude adjustment.

To evaluate the impact of the CalSig on the detection ability of the radar system, we suppose that the radar uses signal coded by maximum length sequences with a pulse compression ratio of 256, the CalSig has a blank ratio M = 32. Figure 15 illustrates signals in a receiving channel.

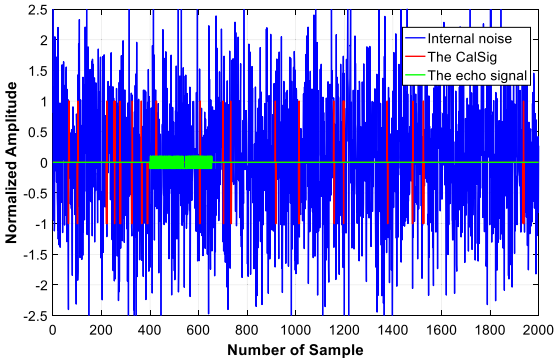

Fig. 15. Illustration of signals in the receiving channel.

The received signal is pulse-compressed in two situations with and without the CalSig, averaged over 32 receiving/transmiting cycles. SNR ratio is calculated in the two cases, giving the reduction of SNR in the case of the CalSig presence. Figure 17 shows the compressed signal. It can be seen that the noise background after the compression filter is higher when the CalSig is applied to the system. Figure 17 indicates the reduction of SNR due to the CalSig, it is approximately 0.13 dB, matching the calculation result. 0.13 dB reduction of SNR causes a decrease of the maximum detection range of the radar by below 1%. Thus, the impact can be neglected.

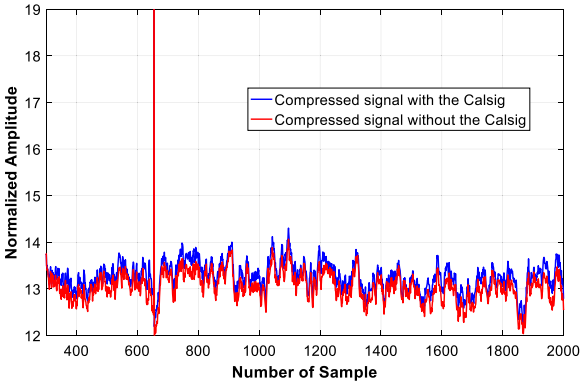

Fig. 16. Compressed signal with and without the CalSig.

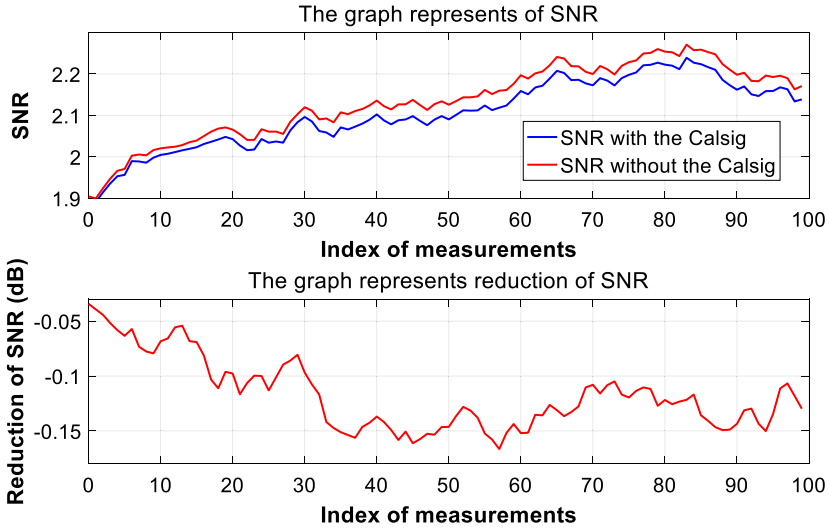

Fig. 17. SNR and reduction of SNR with the CalSig presence.

5 Conclusion

Real-time calibration in radar systems using digital phased array antennas is essential, especially for systems that require high precision in controlling the parameters of the TRMs while the system is in operation. There are various solutions to meet this requirement. In the proposed method, the CalSig frequency is the same operating frequency of the system. The advantage of the method is that the measured parameters reflect more accurately the channel's characteristic, but a big challenge is interference between signals. To overcome the challenge, the CalSig is generated as a random phase-coded signal, simultaneously it is pulse-modulated with a large blank ratio. The proposed calibration method achieves small measurement errors, ensuring real-time requirements and negligible effect on the receive quality of the system. The simulation results show that calibration errors can reach 0.8° and 0.1 dB in phase and amplitude, respectively. The simulation results have demonstrated that calibration errors can reach 0.8° and 0.1 dB in phase and amplitude, respectively. However, as indicated in Figs. 14 and 15, it is easy to see that to reduce measurement errors, we can average through several calibrations (equivalent to increase the number of samples N). This should be done when the system operates stably, if averaging over 16 calibrations the phase and amplitude errors may be less than 0.2° and 0.02 dB.

References

1. Skolnik, M.I.: Radar Handbook, 3rd edn. The McGraw-Hill, New York (2008)
2. Pawlak, H., Charaspreedalarp, A., Jacob, A.F.: Experimental investigation of an external calibration scheme for 30 GHz circularly polarized DBF transmit antenna arrays. In: European Microwave Conference, pp. 764–767. Manchester (2006)

3. Takahashi, T., Konishi, Y., Makino, S., Ohmine, H., Nakaguro, H.: Fast measurement technique for phased array calibration. IEEE Trans. Antennas Propagation **56**(7), 1888–1899 (2008)
4. Pawlak, H., Jacob, A.F.: An external calibration scheme for DBF antenna arrays. IEEE Trans. Antennas Propagation **58**(1), 59–67 (2010)
5. Lee, K.-M., Chu, R.-S., Liu, S.-C.: A built-in Performance-Monitoring Fault Isolation and Correction (PM/FIC) system for active phased-array antennas. IEEE Trans. Antennas Propagation **41**(11), 1530–1540 (1993)
6. Van Werkhaven, G.H.C., Golshayan, A.K.: Calibration aspects of the APAR antenna unit. In: IEEE International Conference on Phased Array Systems and Technology, pp. 425–428. Dana Point, CA (2000)
7. Shipley, C., Woods, D.: Mutual coupling-based calibration of phased array antennas. In: IEEE International Symposium on Phased Array Systems and Technology, pp. 529–532. Dana Point, CA (2000)
8. Fulton, C., Chappell, W.: Calibration techniques for digital phased arrays. In: IEEE International Conference on Microwaves, Communications, Antennas and Electronics Systems, pp. 1–10. Tel Aviv (2009)
9. Aumann, H.M., Fenn, A.J., Willwerth, F.G.: Phased array antenna calibration and pattern prediction using mutual coupling measurements. IEEE Trans. Antennas Propagation **37**(7), 844–850 (1989)
10. Steyskal, H., Herd, J.S.: Mutual coupling compensation in small array antennas. IEEE Trans. Antennas Propagation **38**(12), 1971–1975 (1990)
11. Kim, D., Park, S., Kim, T., Minz, L., Park, S.: Fully digital beamforming receiver with a real-time calibration for 5G mobile communication. IEEE Trans. Antennas Propagation **67**(6), 3809–3819 (2019)
12. Hoffman, J.P., Veilleux, L., Perkovic, D., Peral, E., Shaffer, S.: Digital calibration of TR modules for real-time digital beamforming SweepSAR architectures. In: IEEE Aerospace Conference, pp. 1–8. Big Sky, MT (2012)
13. Horst, S.J., et al.: Implementation of RF circuitry for real-time digital beam-forming SAR calibration schemes. In: IET International Conference, pp. 1–6. Glasgow, UK (2013)
14. Hoffman, J.P., Horst, S., Veilleux, L., Ghaemi, H., Shaffer, S.: Digital calibration system enabling real-time on-orbit beamforming. In: IEEE Aerospace Conference, pp. 1–11. Big Sky, MT (2014)
15. Hoffman, J.P., Horst, S., Ghaemi, H.: Digital calibration system for the proposed NISAR (NASA/ISRO) mission. In: IEEE Aerospace Conference, pp. 1–7. Big Sky, MT (2015)
16. Hoffman, J.: Modular Ku/Ka-band actively calibrated antenna tile. In: IEEE Aerospace Conference, pp. 1–6. Big Sky, MT (2016)
17. Jens, R.: Technique for concurrent internal calibration during data acquisition for SAR systems. Remote Sens. **12**(11) (2020)
18. Standard_deviation Homepage. https://en.wikipedia.org/wiki/Standard_deviation. Accessed 17 Dec 2020